Chemical Science

ROYAL SOCIETY OF CHEMISTRY

EDGE ARTICLE

View Article Online
View Journal | View Issue

Cite this: *Chem. Sci.*, 2020, **11**, 10973

All publication charges for this article have been paid for by the Royal Society of Chemistry

Glycan–glycan interactions determine *Leishmania* attachment to the midgut of permissive sand fly vectors†

Amy R. Hall, ‡[ab] Jamie T. Blakeman, [a] Ahmed M. Eissa, §[c] Paul Chapman,[ad] Ana L. Morales-García, ¶[a] Laura Stennett,‖[e] Oihane Martin,**[e] Emilie Giraud, ††[e] David H. Dockrell, ‡‡[f] Neil R. Cameron, §§[c] Martin Wiese, [g] Laith Yakob, [e] Matthew E. Rogers *[e] and Mark Geoghegan ¶¶[ah]

Received 13th June 2020
Accepted 2nd September 2020

DOI: 10.1039/d0sc03298k

rsc.li/chemical-science

Direct glycan–glycan interactions are increasingly implicated in survival and pathogenicity of bacteria. Here, we show that they can be exploited by protozoan parasites in their insect hosts. Force spectroscopy revealed that *Leishmania* promastigotes display a high-affinity biomolecular interaction between their lipophosphoglycan glycocalyx and mimics of *N*-acetyl-D-galactosamine, commonly expressed on the midguts of a wide range of sand fly vector species. This enabled gut-adhesive nectomonad promastigotes of *Leishmania mexicana* to efficiently bind to membrane-bound mucin-like, O-linked glycoproteins of the sand fly *Lutzomyia longipalpis*, an event crucial for parasite survival, and accounts for a permissive mode of binding. Thus, direct interaction between parasite and sand fly midgut glycans are key to permitting vector competence for all forms of leishmaniasis worldwide. In addition, these studies demonstrate the feasibility of interfering with these interactions as transmission-blocking vaccines.

Introduction

Leishmaniasis is a vector-borne disease caused by protozoa belonging to the genus *Leishmania*, transmitted by the bite of a female phlebotomine sand fly.[1–3] There are few effective drugs against leishmaniasis, many of which are toxic, and over-reliance on them has led to a worldwide rise in drug resistance.[4] Consequently, there is an urgent need to understand the biology and life cycle strategies of these parasites in order to identify new targets for drugs and vaccines.[5]

Of particular interest is the reliance of *Leishmania* on its surface glycoconjugates to anchor themselves to the midgut epithelium of the sand fly.[6] Midgut attachment and directional movement is crucial to *Leishmania* development as it allows the

[a]*Department of Physics and Astronomy, The University of Sheffield, Sheffield S3 7RH, UK*

[b]*Insight SFI Research Centre for Data Analytics, Dublin City University, Glasnevin, Ireland*

[c]*Department of Chemistry, Durham University, Durham DH1 3LE, UK*

[d]*Department of Chemistry, The University of Sheffield, Sheffield S3 7HF, UK*

[e]*Faculty of Infectious and Tropical Diseases, Department of Disease Control, London School of Hygiene and Tropical Medicine, London WC1E 7HT, UK. E-mail: matthew.rogers@lshtm.ac.uk*

[f]*Department of Infection, Immunity & Cardiovascular Disease, The Medical School, The University of Sheffield, Sheffield Teaching Hospitals, Sheffield S10 2RX, UK*

[g]*Strathclyde Institute of Pharmacy and Biomedical Sciences, University of Strathclyde, Glasgow G4 0RE, UK*

[h]*School of Engineering, Newcastle University, Newcastle NE1 7RU, UK*

† Electronic supplementary information (ESI) available: Experimental methods. Force spectroscopy data of *L. mexicana* nectomonads and metacyclics with CA7AE LPG antibody- and glucose-modified AFM tips (approach and retraction curves and force histograms). LPG Western blot analysis. Data containing peak adhesive force output from the force maps; force event data from the multi-peak analysis of *Leishmania mexicana* WT nectomonads; and force event data from the multi-peak analysis of *L. mexicana* WT metacyclics. Illustrative force maps of *L. mexicana* highlighting large peak force interactions (≥0.1 nN) for the interaction with galactose and glucose-modified AFM tips. See DOI: 10.1039/d0sc03298k

‡ Present address: Insight SFI Research Centre for Data Analytics, Dublin City University, Ireland.

§ Present address: Department of Chemistry, University of Warwick, Coventry, UK; Department of Polymers, Chemical Industries Research Division, National Research Centre, Cairo, Egypt

¶ Present address: Procter and Gamble Newcastle Innovation Centre, Newcastle upon Tyne, UK.

‖ Present address: Department of Imaging Chemistry and Biology, King's College London, London, UK.

** Present address: Servicio de Microbiología, Hospital Universitario Ramón y Cajal, Madrid, Spain.

†† Present address: Institut Pasteur, Paris, France.

‡‡ Present address: Centre for Inflammation Research, University of Edinburgh, Edinburgh, UK.

§§ Department of Materials Science and Engineering, Monash University, Clayton, Australia.

¶¶ Present address: School of Engineering, Newcastle University, Newcastle-Upon-Tyne, UK.

parasites to resist expulsion from the sand fly when it defecates, and therefore to persist beyond the initial blood meal phase of infection.[7] Attachment to the sand fly gut is the weakest point in the parasite life cycle; a significant proportion of parasites are lost at this stage and their survival is dependent on a small population of *Leishmania* that anchor themselves successfully.[6,8] Disruption of this phase of parasite development has the potential to form the basis of a transmission-blocking intervention.

Leishmania are digenetic parasites that alternate between vertebrate and sand fly hosts. In the vertebrate, aflagellate amastigote forms reside within macrophages, which are picked up by the sand fly with a blood meal. During colonization of the sand fly, *Leishmania* undergo several morphological transformations as flagellated promastigotes, culminating in the differentiation to a mammal-infective metacyclic form in the anterior midgut, in readiness for transmission.[9] Towards the end of blood meal digestion, elongated nectomonad promastigotes attach to the sand fly midgut epithelia by utilizing lipophosphoglycan (LPG) on their surface. LPG is a tripartite oligosaccharide consisting of a glycosylphosphatidylinositol anchor and a conserved backbone of phosphoglycan (Gal-Man-P) repeat units (6Gal(β1-4)Man(α1)-PO_4-) with an oligosaccharide cap (Scheme 1). The phosphoglycan domain is polymorphic among *Leishmania* species and may be either unsubstituted or variably substituted with phosphoglycosylated oligosaccharide side chains.[10,11] During metacyclogenesis further modification to the LPG occurs, resulting in elongation and, for some *Leishmania* species such as *Leishmania major*, substitution of the oligosaccharide side chains for different sugars.[11] The net result is masking of side chains involved in attachment, ensuring that the metacyclic promastigotes are free within the lumen of the sand fly gut and available for transmission when the sand fly bites again.

The distribution of leishmaniasis is primarily driven by the availability of competent vectors, which can be subdivided into restrictive or permissive vectors depending on their ability to support development of various *Leishmania* species. Variability in the oligosaccharide side chains of LPG has been closely associated with midgut attachment and vector specificity. This high degree of specificity is known to occur for certain parasites with restrictive sand fly hosts such as *L. major* with *Phlebotomus papatasi* and *Leishmania tropica* with *Phlebotomus sergenti*.[12,13] In these vectors, attachment is controlled by LPG receptors that bind to the terminal sugars of the oligosaccharide side chains of the non-metacyclic promastigote stages. In the best characterized example, *P. papatasi*, a midgut-expressed galectin (PpGalec: a β-galactoside binding lectin) mediates attachment to terminal galactose residues presented by LPG on the non-infectious promastigotes of *L. major* and *Leishmania turanica*.[13,14] As a consequence of this close co-evolution between parasite and vector, these sand flies are refractory to the development of other *Leishmania* species. However, the majority of sand fly vectors are more permissive in the range of *Leishmania* species that they are able to support and transmit, including *Leishmania*-sand fly combinations not found in nature.[15] Furthermore, it has been proposed that attachment in these sand flies may not be LPG-driven, as it was observed that LPG-null mutants of *Leishmania mexicana* and *L. major* could colonize the permissive vectors *Lutzomyia longipalpis* and *Phlebotomus arabicus*.[16,17] The New World sand fly *Lu. longipalpis* is the natural vector of *Leishmania infantum*, a causative agent of visceral leishmaniasis. However, studies have shown that it can also support the development of a large number of both Old and New World *Leishmania* species, including, *L. major*, *Leishmania donovani*, *L. mexicana*, *Leishmania braziliensis* and *L. amazonensis*.[9,16,18–20] Despite these observations, the mechanism of *Leishmania* attachment to the midgut of permissive sand fly species remains elusive, yet it would allow new insight into the complex epidemiology of the disease and may offer new targets for interrupting parasite transmission.

Consequently, there is considerable interest in identifying the molecules involved in *Leishmania* attachment to permissive vectors as potential targets for disease control. Glycoproteins, structurally similar to mammalian mucins, that bind to *Helix pomatia* agglutinin (HPA) were found to be common to the midgut microvillar surface of permissive but not specific vectors.[21,22] A protein of a predicted molecular mass of 19 kDa but an apparent molecular mass of 40–45 kDa (by electrophoresis) was identified as the responsible proteoglycan carrying O-glycans containing *N*-acetyl-D-galactosamine (GalNAc).[23] Glycan array analysis has shown that HPA binds to a wide range of glycans, which incorporate galactose in their structure, and that it has a strong affinity for GalNAc.[24,25] Therefore, the galactose/GalNAc-bearing midgut glycoproteins of permissive sand fly vectors could potentially bind to exposed lectins or heparin-binding proteins on the parasite surface.[26,27]

An alternative and unexplored mode of binding for *Leishmania* are direct glycan–glycan interactions between the sugar moieties of LPG and the GalNAc of permissive sand fly midguts. Once considered as providing weak adhesive force for bacteria, recent work has shown that glycan–glycan interactions significantly contribute toward their virulence.[28,29] In this respect, force spectroscopy, a technique related to atomic force microscopy (AFM), can effectively probe the binding of different molecules to individual, live cells in a label-free manner.[30] Moreover, it can explore the

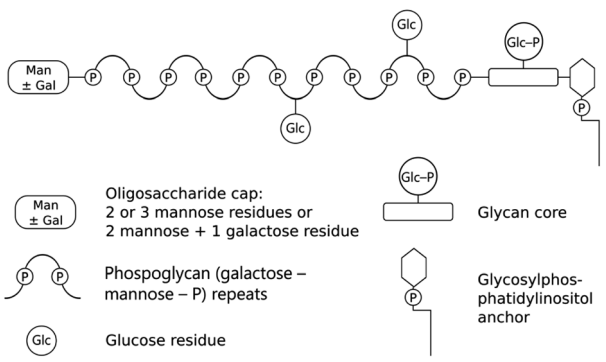

Scheme 1 Structure of *L. mexicana* nectomonad LPG.

distribution of particular molecules on the cell surface with nanometre resolution.[30–32]

To test the direct glycan–glycan interactions hypothesis, force spectroscopy was used to directly measure the strength of adhesion between LPG and a GalNAc-mimicking glycopolymer and to obtain nanoscale information on the localization and distribution of GalNAc-binding molecules on the surface of *L. mexicana* metacyclic and nectomonad promastigotes. To achieve this, AFM tips interacting with the parasite were coated with a galactose (Gal)-bearing synthetic glycopolymer, which acted to mimic multivalent GalNAc glycoproteins. (Lectins generally show significant binding to both Gal and GalNAc.[33,34])

The growth of polymers (brushes) from AFM tips to interrogate physical[35,36] or biological[37] systems has rarely been performed, and the work presented here shows how this approach can be used to understand the molecular roles involved in hosting parasitic pathogens. The results show that the LPG on the surface of gut-adhesive nectomonad promastigotes display high affinity for GalNAc mimics, in the order of adhesion displayed by bacterial pili–protein–mucin interactions. This mode of adhesion was stage-specific and dependent on the presence of LPG on the parasite surface. Moreover, interference with its binding in sand flies reveal it as a potent target for transmission blockade. These force spectroscopy data were used to build a map of the spatial distribution of adhesion,[38,39] which revealed a non-homogeneous distribution for a proportion of parasites, thus contributing to an understanding of the underlying molecular interactions used by *Leishmania* parasites to colonize their sand fly hosts.

Modelling reveals that a transmission-blocking vaccine (TBV) could be effective against leishmaniasis if ligands of high glycan–glycan adhesive force are targeted. Collectively, the current study on the interaction of the protozoan parasite *L. mexicana* with the permissive vector *Lu. longipalpis* provides evidence for the role of highly adhesive glycan–glycan interactions in the establishment of parasites within their insect vectors. This work therefore highlights the value of using a multidisciplinary approach, in which synthetic chemistry, biophysics, and parasitology are used to address a basic biological problem of global medical importance.

Results and discussion

Stage-specificity of the LPG-sand fly interaction

To explore the difference between non-metacyclic and metacyclic LPG for binding to sand fly midguts, *Lu. longipalpis* midguts *ex vivo* were probed with fluorescein isothiocyanate

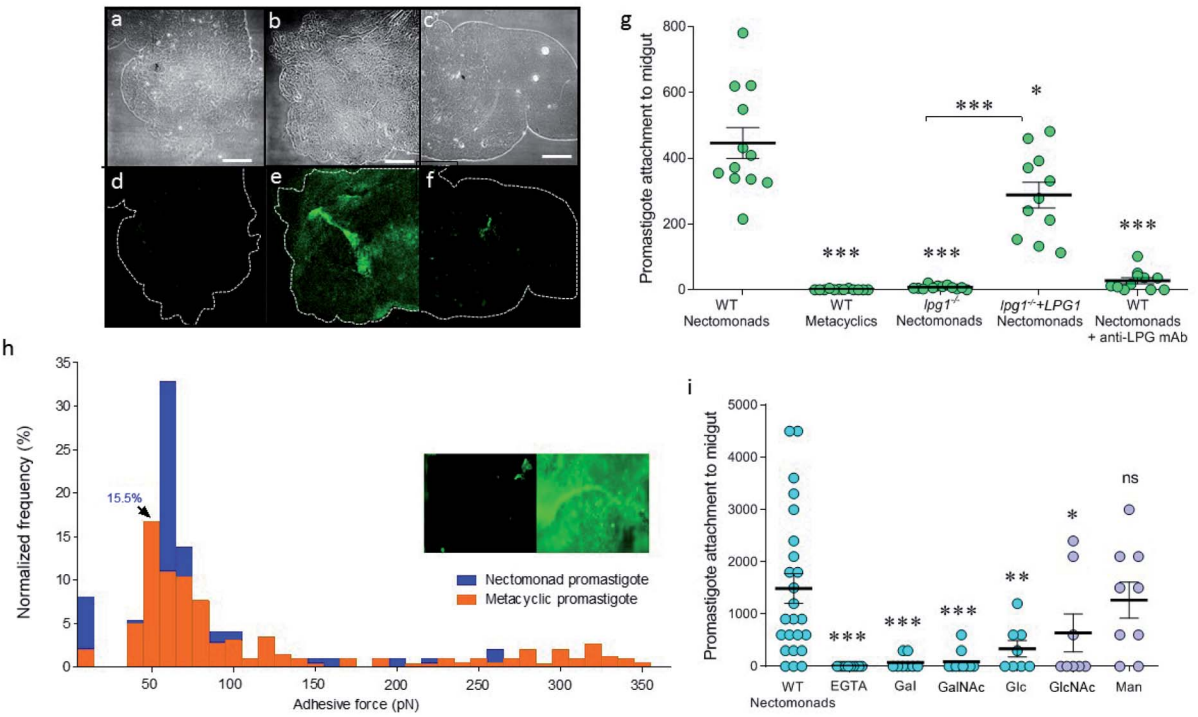

Fig. 1 Stage-specific binding of *L. mexicana* LPG. (a–f) Immunofluorescence of FITC-labelled LPG bound to *Lu. longipalpis* sand fly midguts *ex vivo*. The top panels are phase contrast and the bottom panels immunofluorescence: (a and d) no LPG, (b and e) nectomonad LPG, and (c and f) metacyclic LPG. White scale bars are 100 μm. (g) Midgut attachment of promastigotes of WT, LPG-deficient (*lpg1*$^{-/-}$) and LPG-restored (*lpg1*$^{-/-}$+*LPG1*) mutant *L. mexicana*. (h) Promastigote binding modalities with anti-LPG antibody AFM tips. Typical adhesive force histograms for WT nectomonad (blue) and metacyclic (orange) promastigotes. The inset shows immunofluorescence images of an unfunctionalized and antibody-functionalized AFM tip (left and right panel, respectively), revealing the distribution of anti-LPG mAb. (i) Competition binding assays of WT nectomonad promastigotes for sand fly midguts against different sugars (abbreviations are defined at the end of the article). Solid lines on graphs (g) and (i) represent means ± 1 SEM. Asterisks indicate values that are statistically significant from the WT nectomonad group (ns: not significant, *$p \leq 0.05$, **$p \leq 0.005$, ***$p \leq 0.0005$) using a two-tailed Mann Whitney *t*-test.

(FITC)-labelled LPG, extracted from nectomonad or metacyclic promastigotes of wild type (WT) *L. mexicana* (Fig. 1a–f). Immunofluorescence microscopy confirmed that only LPG from parasites that have not undergone metacyclogenesis could adhere to the vector midgut. This property was replicated in midgut binding assays using live parasites (Fig. 1g). Moreover, mutant parasites deficient in LPG production ($lpg1^{-/-}$) demonstrated that LPG contributed to the midgut binding of this permissive vector species, which was restored by adding back an extra-chromosomal copy of the *LPG1* gene ($lpg1^{-/-}$+*LPG1*). To see if force spectroscopy could be used to interrogate the LPG glycocalyx of *Leishmania*, AFM tips were functionalized with a monoclonal antibody (mAb CA7AE), which recognizes the phosphoglycan (Gal-Man-P) repeat units of the LPG backbone. Typical adhesive force histograms of nectomonad and metacyclic promastigotes show that the majority of binding occurred in the lower range (Fig. 1h). However, metacyclic promastigotes displayed an extended range of stronger binding interactions, such that the average force across all of the parasites was 0.07 ± 0.01 nN for nectomonad promastigotes and 0.18 ± 0.01 nN for metacyclic promastigotes. To test the role of specific sugar moieties present on LPG, midgut-binding assays were conducted (Fig. 1i).

Midgut binding could be competitively inhibited by both galactose and glucose, or their amino-sugar derivatives, GalNAc and GlcNAc but not by mannose. Furthermore, inclusion of ethylene-bis(oxyethylenenitrilo)tetraacetic acid (EGTA) confirmed that attachment is also a calcium-dependent process.

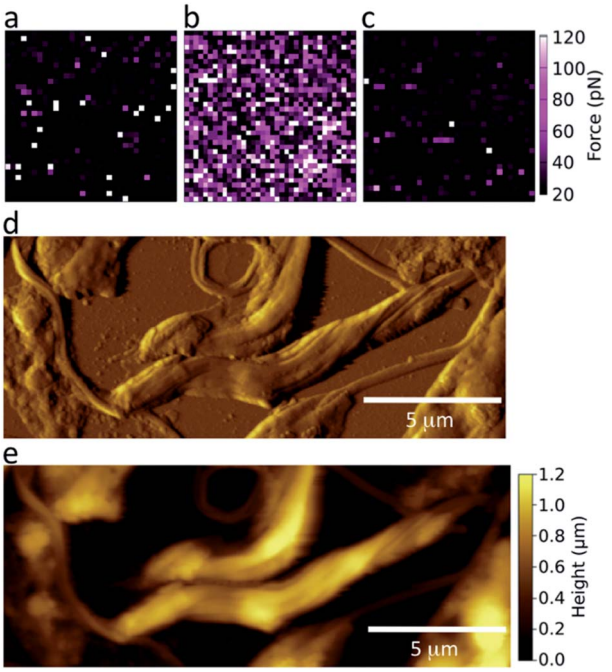

Fig. 2 SFM optimization. Representative force maps of galactose glycopolymer-functionalized AFM tips in PBS against (a) mica (mean adhesion 21 ± 1 pN); (b) mica coated with soybean agglutinin (SBA, 113 ± 2 pN); (c) mica coated with SBA with additional free galactosamine in the imaging buffer (21 ± 1 pN), with the peak adhesive forces stated after each substrate. Representative (d) deflection and (e) height images of WT *L. mexicana* nectomonad promastigotes in air. Although deflection images do not provide quantitative information, they aid in the identification of specific features in topographical images. The force scale applies to the data in (a), (b), and (c).

Force mapping of live parasites

To achieve a GalNAc-mimicking coating, poly(*N*-2-(β-D-galactosyloxy)ethyl methacrylamide) brushes were grown from AFM tips (Scheme S1, ESI†). This coating is chemically similar to GalNAc; the chemical difference (–OH in Gal, –NHAc in GalNAc) occurs adjacent to the polymer backbone, which is unlikely to be accessible to the parasite LPG for stereochemical reasons. To test the specificity of these coated AFM tips and determine their suitability for detecting lectin-like activity on the surface of *Leishmania*, the adhesive force was measured in phosphate buffered saline (PBS) against freshly cleaved mica or immobilized lectin (Fig. 2a and b, respectively). GalNAc-mimicking tips displayed specificity for the GalNAc/Gal-binding lectin soybean agglutinin (SBA);[40] confirmed by loss of adhesion upon the addition of free, competing galactosamine (Fig. 2c).

The surface morphology of nectomonad promastigotes of *L. mexicana* was visualized using scanning force microscopy (SFM). Fig. 2 shows representative deflection (d) and height (e) images taken in air of *L. mexicana* WT nectomonad promastigotes on a glass slide. During adhesion experiments, less detailed height maps were generated from the force curves as contact- or tapping-mode imaging in PBS tended to cause detachment or damage to the parasites. In cases where the parasite body was firmly attached to the substrate, but its flagellum was not, flagellum movement was observed both during and after force mapping, indicating that the parasites were alive during SFM measurements.

Because GalNAc has been described on the luminal surface of permissive sand fly midgut epithelia,[22] GalNAc-mimicking AFM tips were used to map the adhesion for different *L. mexicana* promastigote stages. Fig. 3 shows force maps for the adhesion of (a) metacyclic and (b) nectomonad promastigotes to such tips. From previous microscopy studies of infected sand flies, *Leishmania* promastigotes have been found to orientate their flagella between the microvilli of the sand fly midgut, suggesting that the majority of adhesion occurs between molecules present on the surface of the flagellum and midgut epithelium.[41] Here, promastigotes (nectomonad or metacyclic) did not display adhesive polarity towards galactose across the cell body and flagellum. For the majority of promastigotes, the adhesive molecules required for binding to galactose residues are randomly and evenly distributed across the parasite surface (Fig. 3a, d and f). However, a proportion of both nectomonad and metacyclic promastigotes (36% and 45%, respectively) displayed a line of high adhesive force (>80 pN). Representative images (Fig. 3b and e) show that this region of high adhesion maps to the central axis of the promastigote body but did not occur on the flagellum, raising the possibility of the presence of

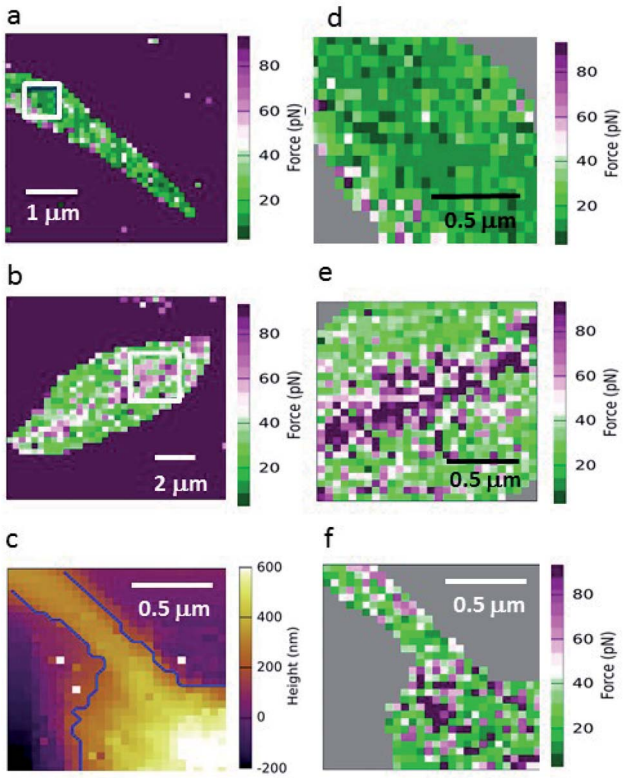

Fig. 3 Representative adhesive force maps of live WT *L. mexicana* promastigote surfaces probed with GalNAc-mimicking AFM tips. Representative force maps of (a) a metacyclic promastigote showing a random distribution of strong binding events and (b) a nectomonad promastigote from the subpopulation that displayed a central region of high adhesive force along the length of the cell body. Higher resolution images of (a) and (b) are shown in the right-hand panels (d) and (e), focusing on a 1.5–2.0 μm^2 area. Typical height (c) and force (f) maps of the anterior of a metacyclic promastigote in higher resolution.

a more adhesive subpopulation of promastigotes during sand fly infection.

Force–distance curves

To assess the range of interactions measured between the nectomonad promastigote surface and galactose, force spectroscopy was performed, with typical adhesion profiles and sample force–distance curves shown in Fig. 4. It can be seen from Fig. 4a that there is a large range in the scale of measured forces for both nectomonad and metacyclic promastigotes probed with a GalNAc-mimicking AFM tip (the average force across all of the parasites was 64 ± 5 pN for nectomonad promastigotes and 42 ± 3 pN for metacyclic promastigotes). This is despite the individual force curves displaying conserved features, such as molecule extension and bond rupture. From these results there is a clear difference in the number of binding events measured on metacyclic promastigotes compared to nectomonad promastigotes. This difference is reflected across all force maps for these two combinations, with metacyclic promastigotes having, on average, almost twice the number of force curves in a map containing no adhesive events as nectomonad promastigotes (75 ± 5% compared to 39 ± 5%, Fig. 4b). Furthermore, multiple binding events were over ten times more frequent on the surface of nectomonad promastigotes compared to metacyclic promastigotes (proportion of force maps with three or more binding events was 5 ± 1% for nectomonad promastigotes and 0.3 ± 0.2% for metacyclic promastigotes), suggesting that ligands, which have multivalent adhesion properties, are likely to be more densely aggregated on nectomonad promastigotes.[42] (The anti-LPG mAb CA7AE on the other hand rarely exhibited multiple adhesion events, possibly due to it being adsorbed to the AFM tip rather than extending into the medium.) To put this mode of binding in context, and accepting that there will be variations between experimental conditions, the average binding affinity of *L. mexicana* nectomonad LPG for GalNAc is comparable to other protein–glycan interactions between bacterial pili and mucins;[43,44] bacterial pili and host pneumocytes;[45] bacterial adhesins;[46–48] and soybean agglutinin and porcine gastric mucin,[49] and greater than a range of glycan–glycan interactions recorded within self-assembling mucins.[50–52]

Sample force curves showing extension and rupture of single and multiple bonds between functionalized AFM tips and a strongly adhesive WT *L. mexicana* nectomonad promastigote are shown in Fig. 4c and d, respectively. These multiple binding events illustrate that strong adhesion between the nectomonad promastigote surface and GalNAc residues on the sand fly gut may be a result of LPG or LPG-like molecules that bear numerous binding sites, such as membrane proteophosphoglycan (mPPG), or dense concentrations of ligands with single, strongly interacting binding sites (Fig. 4e). mPPG is predicted to be 300–400 nm long and therefore to extend beyond the dense 15 nm LPG glycocalyx.[53] This makes mPPG a highly accessible ligand for binding partners and potentially important for sand fly midgut attachment. It could also account for the long extension before a number of binding events on both nectomonad (up to 0.83 ± 0.04 μm) and metacyclic promastigotes (up to 0.64 ± 0.05 μm), with 50% of events occurring at extensions in the range 100–260 nm for both types of promastigote. Measured extension distances are only approximate because both the length and the position of the interacting residue on the glycopolymer-coated AFM tip contribute to this distance. Although the number of mPPG molecules on promastigotes (all life cycle stages) is much less than that of LPG,[53] a single mPPG molecule provides many more potential receptor-binding sites, because it displays leucine-rich repeat units and carries up to 800 serine-linked LPG-like phosphoglycan chains clustered in a specific domain, whereas LPG carries just one.[53] Despite this, LPG-deficient *L. mexicana* promastigotes retain their ability to synthesize and incorporate mPPG on their surface.[54] This argues that the majority of midgut binding and adhesive force to GalNAc on the parasite surface is provided by LPG.

LPG is known to be the dominant parasite ligand for midgut binding in restrictive sand fly species.[55,56] However, its role in midgut attachment in permissive sand flies is less well defined. LPG-deficient mutants of *L. mexicana* and *L. major* have been shown to survive, albeit slightly less efficiently, in permissive sand flies such as *Lu. longipalpis* and *Phlebotomus*

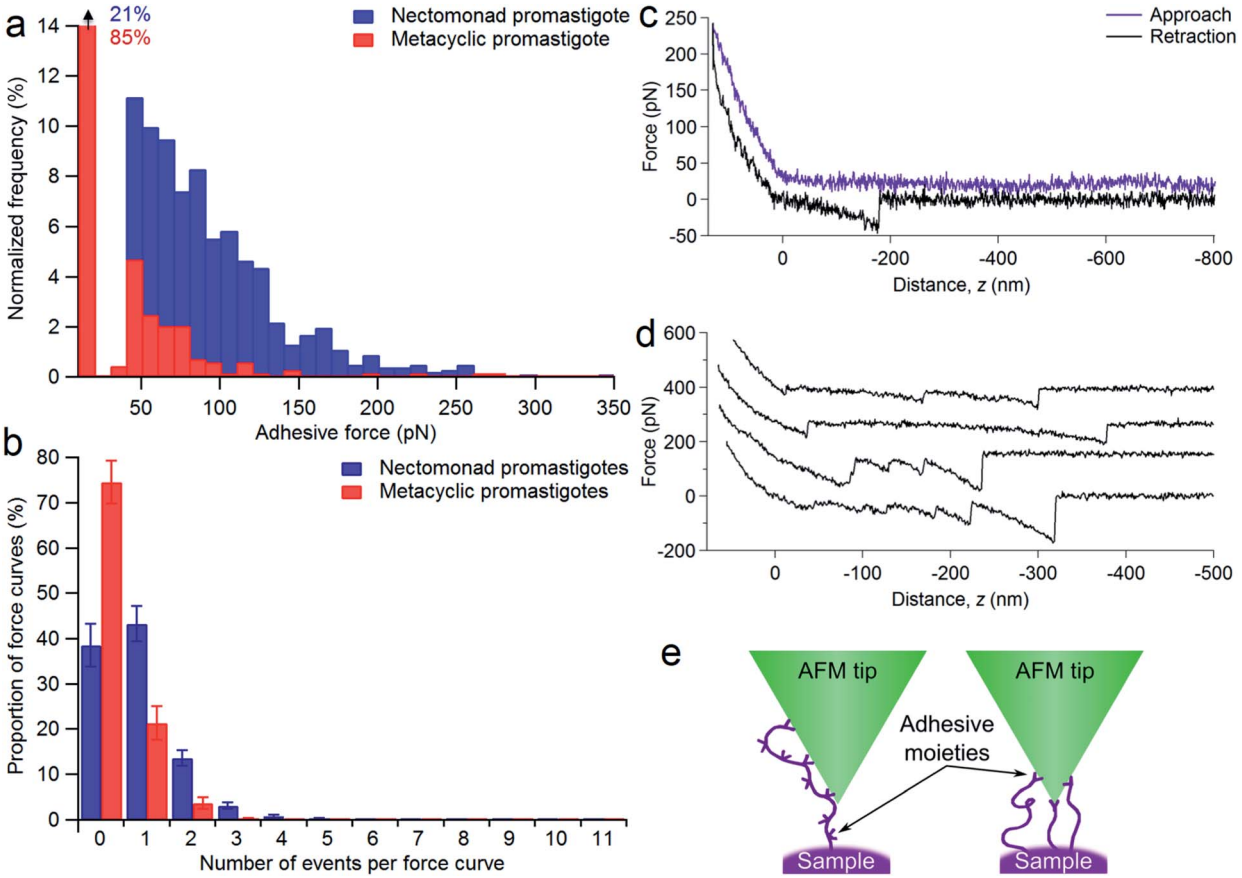

Fig. 4 *L. mexicana* promastigote binding modalities with galactose AFM tips. (a and b) Typical adhesive force histograms for a WT nectomonad (blue) and metacyclic (red) promastigote. (c and d) Force–distance curves for a WT nectomonad promastigote showing examples of (c) the forces measured as the glycopolymer-coated AFM tip moves towards (approach) and away from (retraction) the parasite, and (d) four examples of retraction curves containing multiple binding events (cropped to 500 nm). These have been offset for clarity; $z = 0$ corresponds to zero force on the cantilever. (e) Schematic diagram of different types of multiple parasite biomolecule-AFM tip interactions that would result in three measured adhesion events. For clarity, the glycopolymer tip-coating has not been included.

perniciosus.[16,17,22,55,57] However, LPG-deficient *L. infantum* demonstrated poor development in *P. perniciosus*, a natural vector for this parasite in the western Mediterranean, and weak attachment to *ex vivo* midguts of this sand fly compared to WT parasites.[55] A similar result was also recorded for LPG-deficient *L. donovani* and the permissive, Indian vector of this parasite, *Phlebotomus argentipes*.[8] Collectively, these results suggest that there is a degree of dependency on LPG to support the development of some species of *Leishmania* in permissive sand fly vectors. If so, an absence of LPG would reduce the adhesion between the surface of *L. mexicana* nectomonad promastigotes and GalNAc.

Using mutant *L. mexicana* deficient for LPG (*lpg1*$^{-/-}$) and its addback (*lpg1*$^{-/-}$+*LPG1*) alongside WT nectomonad and metacyclic promastigotes, force–distance curves were obtained with coated AFM tips. Analysis of these force–distance curves confirmed the earlier observation (Fig. 5a and b) that there is stage-specific binding to GalNAc (and GlcNAc, *N*-acetyl-D-glucosamine, Fig. S2†), such that WT metacyclic promastigotes displayed 75% less adhesive force over the same area compared to nectomonad promastigotes (4 ± 1 nN μm^{-2} compared to 16 $\pm$ 2 nN μm^{-2} for peak adhesive forces > 20 pN, $p = 0.00008$; Fig. 5a). This was further highlighted when only strong-interaction events (defined here as those with a peak adhesive force > 100 pN) were considered (Fig. 5b). Under these conditions metacyclic promastigotes were ~95% weaker at adhering to coated AFM tips (0.2 ± 0.1 nN μm^{-2} compared to 5 ± 2 nN μm^{-2}, $p = 0.0002$). This is significant and although the structure of *L. mexicana* metacyclic LPG is currently unknown, it is likely to be structurally and chemically modified compared to that of *L. mexicana* nectomonad LPG, as in other *Leishmania* species.

The inability of metacyclic promastigotes or purified metacyclic LPG from *L. mexicana* to bind to *Lu. longipalpis* midguts (Fig. 1a–g), and the presence of higher adhesive force to anti-LPG mAb-AFM tips (Fig. 1h) are consistent with molecular changes to LPG during metacyclogenesis.[6,11,56] In the absence of LPG, the adhesion between the *L. mexicana* nectomonad promastigote surface and galactose was very weak, with a reduction of ~83% (2.8 ± 0.6 nN μm^{-2} compared to 16 ± 2 nN μm^{-2}, $p = 0.00007$) and 99% (0.03 ± 0.02 nN μm^{-2} compared to 5 ± 2 nN μm^{-2}, $p = 0.00001$), for peak adhesive forces > 20 pN and

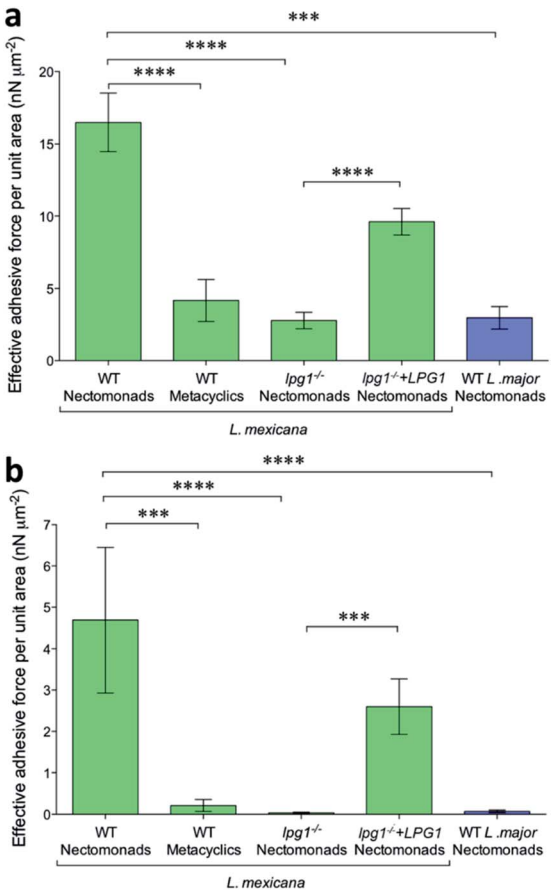

Fig. 5 Influence of *L. mexicana* promastigote life cycle stage and LPG on adhesion to GalNAc mimics. Effective areal adhesive force (±1 SEM) of WT *L. mexicana* nectomonad and metacyclic promastigotes, LPG-deficient (*lpg1*$^{-/-}$) and LPG-restored (*lpg1*$^{-/-}$+*LPG1*) mutant *L. mexicana* nectomonad promastigotes for GalNAc-mimicking galactose-coated AFM tips. WT *L. major* nectomonad promastigotes are shown as a negative control. (a) All adhesive forces (peak adhesive force > 20 pN); (b) strong-interaction forces (peak adhesive forces > 100 pN). Asterisks indicate values that are statistically significant from the WT nectomonad group (***$p \leq 0.001$, ****$p \leq 0.0001$) using a two-tailed Mann Whitney *t*-test.

strongly-interacting binding events (peak adhesive forces > 100 pN), respectively. Furthermore, binding was significantly restored by LPG complementation in the LPG-deficient strain. In contrast, *L. major* WT nectomonad promastigotes displayed poor adhesion to functionalized AFM tips, highlighting that GalNAc/galactose binding cannot be generalized to all *Leishmania* species. Rather, this reinforces the finding that *L. major* relies upon a galectin on the sand fly midgut to resist blood meal defecation and persist in the restrictive sand fly species *P. papatasi*.

The clear decreases in the adhesive force measured and number of events recorded for metacyclic promastigotes compared to their nectomonad counterparts indicate the importance of identifying the specific ligands responsible for the binding in the force spectroscopy experiment. (It is possible that specific interactions in the anti-LPG mAb experiments are present but that they are masked by non-specific interactions.) The decrease in the primary adhesive force is by a factor of four, which is not large and perhaps explains why initial attachment of the parasite to the midgut is often ineffective. This suggests that attempts to inhibit attachment could be a fruitful area of research for novel control strategies.

An interesting finding of this study was the discovery of a line of high adhesive force along the central cell body axis to the GalNAc-mimicking tips. Remarkably, this was found in 36% of nectomonad promastigotes and 45% of metacyclic promastigotes. The precise orientation of *Leishmania* promastigotes for optimal attachment within the midgut is unknown, however; *Leishmania* promastigotes have been found with their flagellum inserted between microvilli.[58] *Leishmania* promastigotes pull themselves through media flagellum first. Video microscopy of *L. mexicana* promastigotes in culture has demonstrated that *Leishmania* encounter surfaces flagellar tip-first, which is promoted by the shape of the cell body. *In silico* modelling revealed that promastigotes with larger cell bodies, such as the gut-adhesive nectomonad promastigotes, can cause considerable drag, resulting in the reorientation of the flagellar tip back to a surface.[59] It is possible therefore that a concentration of high adhesive forces along the cell body may add to this drag effect, enabling the flagellum to dock between the midgut microvilli more successfully. One may also speculate these are the minority of promastigotes that successfully resist defecation of the blood meal remnant by binding to the midgut and go on to colonize the rest of the sand fly for transmission. In future studies, analysis of this subpopulation of promastigotes using force spectroscopy may be revealing.

Although metacyclic promastigotes do not adhere to the sand fly midgut in *ex vivo* gut-binding assays, the line of high adhesion on their surface may be related to their preadaptation for survival in the vertebrate host, to facilitate attachment and entry into their host cell *via* phagocytosis. However, there may be a function for the line of high adhesion within the sand fly, as it has recently been found that a proportion of metacyclics dedifferentiate back into multiplicative promastigotes when they come into contact with blood.[60] It is possible that those metacyclics with the line of high adhesion weakly attach to the sand fly midgut, anchoring them sufficiently to resist being transmitted by regurgitation during a blood meal. After blood intake, these metacyclics would then be able to undergo dedifferentiation to propagate the infectiousness of the sand fly.

Modelling impact of interfering with LPG–GalNAc binding on transmission

Herein, the difference in adhesion between nectomonad and metacyclic promastigotes is shown to be relatively small. This comes from two pieces of evidence: first, we observed that nectomonad promastigotes have an average adhesion ~4 times greater than that for metacyclic promastigotes (Fig. 5a) and second, metacyclic promastigotes have very few large adhesion peaks (adhesion > 100 pN). The nectomonad promastigotes do have large adhesion peaks, but if lower adhesion curves are not considered (Fig. 5b), the areal force decreases by a factor of four. Collectively, this indicates that only a small change is needed to

disrupt adhesion. There is presently considerable uncertainty as to the ease with which nectomonads can successfully attach to the sand fly midgut. In one study, infections using defined doses of *L. mexicana* amastigotes fed to *Lu. longipalpis via* a membrane revealed that three days later 21 parasites successfully resisted blood meal defecation from a population of 1056 promastigotes present just prior to defecation (98% loss).[61] Moreover, a different *Leishmania*-sand fly combination was also reported to lose up to 98% of the parasite load during defecation.[60] Recently, *P. papatasi* sand flies were shown to naturally pick up 80 *L. major* amastigotes from the footpads of infected mice,[60] indicating that the number of parasites that anchor the infection during defecation is likely to be much smaller, further highlighting this critical weakness in the *Leishmania* life cycle. We hypothesize that parasite adherence to the sand fly is dominated by a subpopulation with the necessary ability. For the data presented here, averaged over all *L. mexicana* WT nectomonads (data in ESI†), 9.2% of pixels show high adhesive force > 100 pN. Considering individual parasites, of twelve nectomonads measured, two had force events greater than 100 pN over 24% (*e.g.*, the histogram in Fig. 4a) and 36% of the pixels used and one had fewer than 1%. It is therefore proposed that sand fly midgut adhesion is dominated by a highly adhesive subpopulation rather than by stochastic events. It is therefore reasonable to consider targeting this subpopulation with a transmission-blocking vaccine for those *Leishmania* that either cycle exclusively between humans, such as *L. donovani* transmitted by the permissive sand fly vector, *Phlebotomus argentipes*; or those *Leishmania* where the animal reservoir is defined and can be easily vaccinated such as dogs infected with *L. infantum*, transmitted by the permissive sand fly vector *Lu. longipalpis*.

A transmission-blocking vaccine that impedes adhesion of promastigotes to the sand fly midgut will have several effects on vector life history as well as parasite development. Complete elimination of adhesion will block transmission of the parasite, but the impact on transmission of the more realistic scenario of partial blocking is less clear. For example, partial blocking may reduce the parasite development rate, but it would also reduce fitness costs to the sand fly associated with heavier parasite infections. A simple transmission model is used to project the net impact of partial midgut blocking on *Leishmania* transmission. This model is based on the standard Ross–Macdonald equation for calculating the transmission potential of a vector-borne pathogen,

$$V = \frac{a}{m}\exp(-\tau m), \quad (1)$$

where V is the vectorial capacity, which is a vector-centric measure of transmission potential;[62] a is the probability that a sand fly becomes infected when ingesting a parasitic blood meal; τ is the extrinsic incubation period (EIP) for the parasite (the time taken for the vector to become infectious following its infection); and m is the sand fly mortality rate, so that $1/m$ is the average sand fly lifespan. Infection experiments can be used to parameterize this model. Fitting a logarithmic function to published data[63] results in the following relationship between infective dose (I_D) and the proportion of sand flies becoming colonized,

$$a = 0.086 \ln(I_D) - 0.114. \quad (2)$$

The relationship between infective dose and consequent metacyclics (MET) was also fitted to these data, yielding $\mathrm{MET} = 167\, I_D^{0.32}$.

To calculate the EIP, we used data on the percentage of sand flies carrying metacyclics on day 10 following inoculation with a wide range of infective doses.[63] Of those that received the lowest $I_D = 2 \times 10^3$, 47% were metacyclic-positive at day 10, corresponding to an average EIP of $\tau = 12.5$ d. Of those that received the largest $I_D = 5 \times 10^5$, 92% were metacyclic-positive at day 10, only requiring an average EIP of 3.3 d. Hence, 3.3 and 12.5 d defined the range of EIP whereby lower infective doses prolonged the delay until metacyclic development.

Earlier work[64] demonstrated that higher parasite loads incur a considerable fitness burden on sand flies. Over a range of parasite burdens comparable with the earlier EIP experiments,[63] it was found that sand fly mortality increased approximately linearly with parasite load, ranging from 3 d (heavily infected fly) to 7 d (uninfected fly). Although it is more likely that metacyclics were responsible for the additional mortality it is currently unclear whether this cost to the sand fly is associated with metacyclic or amastigote burden. Therefore, both scenarios were modelled: m was varied to allow for an average sand fly lifespan between 7 and 3 d according to amastigote burden (Fig. 6a) or metacyclic burden (Fig. 6b). In the scenario whereby sand fly mortality increases as a function of amastigote burden (*i.e.* infective dose), blocking adhesion (*e.g.*, through use of a TBV) had an intuitive relationship with transmission: a TBV with 33% and 66% efficacy reduced transmission (vectorial capacity) by approximately one- and two-thirds, respectively. However, if sand fly mortality is a function of metacyclic burden, the projected impact of a TBV is more complicated. Fig. 6b shows that when infective dose is high, imperfect vaccines (efficacy of 33% or 66%) risk

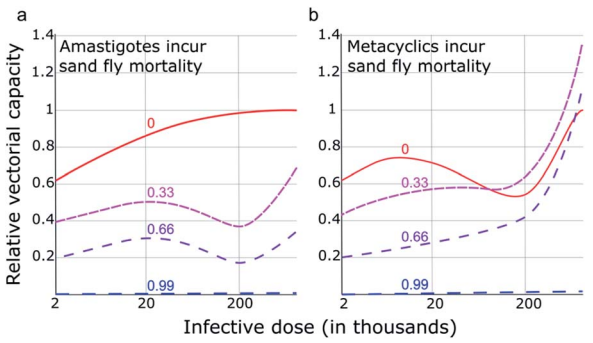

Fig. 6 The modelled impact of a transmission-blocking vaccine (efficacy corresponding with line labels: 0, 0.33, 0.66, 0.99) on the relative vectorial capacity of the sand fly for transmitting *Leishmania*. Higher infective doses of parasites generally lead to higher vectorial capacity. Sand fly mortality is modelled to increase as a function of (a) the infectious dose or (b) metacyclic numbers.

exacerbating vectorial capacity. This is because, even though parasite development from amastigote to metacyclic form is partially blocked, the consequently reduced metacyclic-associated sand fly mortality more than offsets this blockade. Meaning, in transmission settings where the average infective dose is high, a TBV that has less than approximately 66% efficacy could pose a health risk.

Conclusions

LPG has been shown to be responsible for stage-specific adhesion of *L. mexicana* nectomonad promastigotes to GalNAc; an epitope found in a mucin-like glycoprotein, coating permissive sand fly midguts. These results indicate that LPG-dependent and independent mechanisms operate side-by-side in permissive vectors and that LPG adhesion is mediated by relatively few high-force glycan–glycan interactions. In our model of permissive sand fly attachment, the presence of free GalNAc resulted in a significant decrease in promastigote binding. This is strong evidence that GalNAc provides an essential substrate for midgut attachment, mediated through glycan–glycan interactions. Modelling indicates that targeting such midgut attachment mechanisms is a viable transmission-blocking strategy against leishmaniasis. Furthermore, the work has demonstrated that the growth of polymer brushes decorated with specific moieties as a means of interrogating microorganisms is a viable strategy for understanding specific interactions. This technology is versatile and is likely to be applicable in the study of parasite–vector interactions beyond that of *Leishmania* with its sand fly host. Furthermore, there is scope for development in other areas, for example by tethering antiparasitics or antibiotics to the brush.

Author contributions

MER, ARH, MG, and NRC conceived and designed the experiments; ARH, JTB, MER, AME, PC, LS, OM, and EG performed the experiments; ARH, ALMG, JTB, and MG analysed the force spectroscopy data; LY performed the modelling; MW provided *Leishmania* mutant cell lines; MG, MER, and DHD supervised the work; ARH, LY, MER, and MG wrote the paper, to which all authors contributed and which all authors have approved.

Conflicts of interest

There are no conflicts of interest to declare.

Abbreviations

AFM	Atomic force microscopy
EGTA	Ethylene-bis(oxyethylenenitrilo)tetraacetic acid
EIP	Extrinsic incubation period
FITC	Fluorescein isothiocyanate
Gal	Galactose
GalNAc	*N*-acetyl-D-galactosamine
Glc	Glucose
GlcNAc	*N*-acetyl-D-glucosamine
HPA	*Helix pomatia* agglutinin
LPG	Lipophosphoglycan
mAb	Monoclonal antibody
Man	Mannose
mPPG	Membrane proteophosphoglycan
PBS	Phosphate buffered saline
SEM	Standard error of the mean
SFM	Scanning force microscopy
SBA	Soybean agglutinin
TBV	Transmission-blocking vaccine
WT	Wild-type

Acknowledgements

MG thanks Prof. Michel Bergeron (Université Laval) for the suggestion of *Leishmania*. MG and MER acknowledge Prof. Steve Brocchini (UCL: University College London) for the introduction. ARH acknowledges Prof. David Alsteens (UCL: Université Catholique de Louvain) for useful discussions. MER and EG were supported by the BBSRC (David Phillips Fellowship awarded to MER, BB/H022406/1) and MER also acknowledges the BBSRC for support of LS through a London Interdisciplinary Doctoral Programme rotation project; LY and MER acknowledge funding from the MRC through the VALIDATE programme (MR/R005850/1); OM was supported by the Basque Government (Fellowship BF109.183); AME was supported by the Leverhulme Trust (F/00128/BO); PC and ALMG were supported by the EPSRC (EP/I012060/1) and ALMG also acknowledges CONACyT for a doctoral studentship; and ARH and JTB by the EPSRC through respectively a doctoral training grant and iCASE award associated with the doctoral training centre in polymers, soft matter, and colloids. Nuria Melisa Morales-García is gratefully acknowledged for using her skill in BioRender to provide a table-of-contents graphic.

Notes and references

1 J. Alvar, I. D. Vélez, C. Bern, M. Herrero, P. Desjeux, J. Cano, J. Jannin, M. den Boer, D. Argaw, S. Bhattacharya, M. Ejov, A. N. Elkhouri, J. A. Ruiz-Postigo and J. Serrano, *PLoS One*, 2012, **7**, e35671.
2 P. A. Bates, *Int. J. Parasitol.*, 2007, **37**, 1097–1106.
3 World Health Organization, *Control of the Leishmaniases*, WHO, Geneva, 2010.
4 A. S. Nagle, S. Khare, A. B. Kumar, F. Supek, A. Buchynskyy, C. J. N. Mathison, N. K. Chennamaneni, N. Pendem, F. S. Buckner, M. H. Gelb and V. Molteni, *Chem. Rev.*, 2014, **114**, 11305–11347.
5 S. L. Croft and P. Olliaro, *Clin. Microbiol. Infect.*, 2011, **17**, 1478–1483.
6 D. Sacks and S. Kamhawi, *Annu. Rev. Microbiol.*, 2001, **55**, 453–483.
7 T. Beneke, F. Demay, E. Hookway, N. Ashman, H. Jeffery, J. Smith, J. Valli, T. Becvar, J. Myskova, T. Lestinova,

S. Shafiq, J. Sadlova, P. Volf, R. J. Wheeler and E. Gluenz, *PLoS Pathog.*, 2019, e1007828.
8 D. L. Sacks, G. Modi, E. Rowton, G. Spath, L. Epstein, S. J. Turco and S. M. Beverley, *Proc. Natl. Acad. Sci. U. S. A.*, 2000, **97**, 406–411.
9 M. E. Rogers, M. L. Chance and P. A. Bates, *Parasitology*, 2002, **124**, 495–507.
10 R. R. de Assis, I. C. Ibraim, P. M. Nogueira, R. P. Soares and S. J. Turco, *Biochim. Biophys. Acta*, 2012, **1820**, 1354–1365.
11 C.-L. Forestier, Q. Gao and G.-J. Boons, *Front. Cell. Infect. Microbiol.*, 2014, **4**, 193.
12 S. Kamhawi, G. B. Modi, P. F. P. Pimenta, E. Rowton and D. L. Sacks, *Parasitology*, 2000, **121**, 25–33.
13 S. Kamhawi, M. Ramalho-Ortigao, V. M. Pham, S. Kumar, P. G. Lawyer, S. J. Turco, C. Barillas-Mury, D. L. Sacks and J. G. Valenzuela, *Cell*, 2004, **119**, 329–341.
14 P. Volf, P. M. Nogueira, J. Myskova, S. J. Turco and R. P. Soares, *Parasitol. Int.*, 2014, **63**, 683–686.
15 P. Volf and J. Myskova, *Trends Parasitol.*, 2007, **23**, 91–92.
16 M. E. Rogers, T. Ilg, A. V. Nikolaev, M. A. J. Ferguson and P. A. Bates, *Nature*, 2004, **430**, 463–467.
17 A. Svárovská, T. H. Ant, V. Seblová, L. Jecná, S. M. Beverley and P. Volf, *PLoS Neglected Trop. Dis.*, 2010, **4**, e580.
18 P. Cecílio, A. C. A. M. Pires, J. G. Valenzuela, P. F. P. Pimenta, A. Cordeiro-da-Silva, N. F. C. Secundino and F. Oliveira, *J. Infect. Dis.*, 2020, **222**, 1199–1203.
19 J. S. P. Doehl, Z. Bright, S. Dey, H. Davies, J. Magson, N. Brown, A. Romano, J. Dalton, A. I. Pinto, J. W. Pitchford and P. M. Kaye, *Nat. Commun.*, 2017, **8**, 57.
20 P. M. Nogueira, A. C. Guimarães, R. R. Assis, J. Sadlova, J. Myskova, K. Pruzinova, J. Hlavackova, S. J. Turco, A. C. Torrecilhas, P. Volf and R. P. Soares, *Parasites Vectors*, 2017, **10**, 608.
21 L. G. Evangelista and A. C. R. Leite, *J. Med. Entomol.*, 2002, **39**, 432–439.
22 J. Myskova, M. Svobodova, S. M. Beverley and P. Volf, *Microbes Infect.*, 2007, **9**, 317–324.
23 J. Myšková, A. Dostálová, L. Pěničková, P. Halada, P. A. Bates and P. Volf, *Parasites Vectors*, 2016, **9**, 413.
24 M. A. Haseeb, C. Thors, E. Linder and L. K. Eveland, *Exp. Parasitol.*, 2008, **119**, 67–73.
25 A. Markiv, D. Peiris, G. P. Curley, M. Odell and M. V. Dwek, *J. Biol. Chem.*, 2011, **286**, 20260–20266.
26 E. de Almeida Marques da Silva and T. V. Fialho Martins, *J. Glycobiol.*, 2016, **5**, 1000120.
27 L. M. de Castro Côrtes, M. C. de Souza Pereira, F. S. da Silva, B. A. Pereira, F. O. de Oliveira Junior, R. O. de Araújo Soares, R. P. Brazil, L. Toma, C. M. Vicente, H. B. Nader, M. de Fátima Madeira, F. J. Bello and C. R. Alves, *Parasites Vectors*, 2012, **5**, 142.
28 C. J. Day, E. N. Tran, E. A. Semchenko, G. Tram, L. E. Hartley-Tassell, P. S. K. Ng, R. M. King, R. Ulanovsky, S. McAtamney, M. A. Apicella, J. Tiralongo, R. Morona, V. Korolik and M. P. Jennings, *Proc. Natl. Acad. Sci. U. S. A.*, 2015, **112**, E7266–E7275.
29 C. Formosa-Dague, M. Castelain, H. Martin-Yken, K. Dunker, E. Dague and M. Sletmoen, *Microorganisms*, 2018, **6**, 39.
30 Y. F. Dufrêne, *mBio*, 2014, **5**, e01363.
31 D. Alsteens, M. C. Garcia, P. N. Lipke and Y. F. Dufrêne, *Proc. Natl. Acad. Sci. U. S. A.*, 2010, **107**, 20744–20749.
32 L. Arnal, G. Longo, P. Stupar, M. F. Castez, N. Cattelan, R. C. Salvarezza, O. M. Yantorno, S. Kasas and M. E. Vela, *Nanoscale*, 2015, **7**, 17563–17572.
33 V. S. R. Rao, K. Lam and P. K. Qasba, *J. Biomol. Struct. Dyn.*, 1998, **15**, 853–860.
34 V. Sharma, V. R. Srinivas, P. Adhikari, M. Vijayan and A. Surolia, *Glycobiology*, 1998, **8**, 1007–1012.
35 M. Raftari, Z. J. Zhang, S. R. Carter, G. J. Leggett and M. Geoghegan, *Macromolecules*, 2015, **48**, 6272–6279.
36 M. Raftari, Z. J. Zhang, S. R. Carter, G. J. Leggett and M. Geoghegan, *Tribol. Lett.*, 2018, **66**, 11.
37 P. Schön, E. Kutnyanszky, B. ten Donkelaar, M. G. Santonicola, T. Tecim, N. Aldred, A. S. Clare and G. J. Vancso, *Colloids Surf., B*, 2013, **102**, 923–930.
38 V. Dupres, F. D. Menozzi, C. Locht, B. H. Clare, N. L. Abbott, S. Cuenot, C. Bompard, D. Raze and Y. F. Dufrêne, *Nat. Methods*, 2005, **2**, 515–520.
39 A. R. Hall and M. Geoghegan, *Rep. Prog. Phys.*, 2018, **81**, 036601.
40 H. Lis, B.-A. Sela, L. Sachs and N. Sharon, *Biochim. Biophys. Acta*, 1970, **211**, 582–585.
41 L. L. Walters, G. B. Modi, R. B. Tesh and T. Burrage, *Am. J. Trop. Med. Hyg.*, 1987, **36**, 294–314.
42 H. Handa, S. Gurczynski, M. P. Jackson and G. Mao, *Langmuir*, 2010, **26**, 12095–12103.
43 A. P. Gunning, D. Kavanaugh, E. Thursby, S. Etzold, D. A. MacKenzie and N. Juge, *Int. J. Mol. Sci.*, 2016, **17**, 1854.
44 P. Tripathi, A. Beaussart, D. Alsteens, V. Dupres, I. Claes, I. von Ossowski, W. de Vos, A. Palva, S. Lebeer, J. Vanderleyden and Y. F. Dufrène, *ACS Nano*, 2013, **7**, 3685–3697.
45 A. Beaussart, A. E. Baker, S. L. Kuchma, S. El-Kirat-Chatel, G. A. O'Toole and Y. F. Dufrêne, *ACS Nano*, 2014, **8**, 10723–10733.
46 O. Björnham, J. Bugaytsova, T. Borén and S. Schedin, *Biophys. Chem.*, 2009, **143**, 102–105.
47 O. Björnham, E. Fällman, O. Axner, J. Ohlsson, U. J. Nilsson, T. Borén and S. Schedin, *J. Biomed. Opt.*, 2005, **10**, 044024.
48 K. H. Simpson, G. Bowden, M. Höök and B. Anvari, *J. Bacteriol.*, 2003, **185**, 2031–2035.
49 M. Sletmoen, T. K. Dam, T. A. Gerken, B. T. Stokke and C. F. Brewer, *Biopolymers*, 2009, **91**, 719–728.
50 K. E. Haugstad, T. A. Gerken, B. T. Stokke, T. K. Dam, C. F. Brewer and M. Sletmoen, *Biomacromolecules*, 2012, **13**, 1400–1409.
51 K. E. Haugstad, S. Hadjialirezaei, B. T. Stokke, C. F. Brewer, T. A. Gerken, J. Burchell, G. Picco and M. Sletmoen, *Glycobiology*, 2016, **26**, 1338–1350.
52 C. Tromas, J. Rojo, J. de la Fuente, A. Barrientos, R. García and S. Penadés, *Angew. Chem., Int. Ed.*, 2001, **40**, 3052–3055.

53 T. Ilg, *Parasitol. Today*, 2000, **16**, 489–497.
54 T. Ilg, *EMBO J.*, 2000, **19**, 1953–1962.
55 L. Jecna, A. Dostalova, R. Wilson, V. Seblova, K.-P. Chang, P. A. Bates and P. Volf, *Parasitology*, 2013, **140**, 1026–1032.
56 D. L. Sacks, *Cell. Microbiol.*, 2001, **3**, 189–196.
57 N. Secundino, N. Kimblin, N. C. Peters, P. Lawyer, A. A. Capul, S. M. Beverley, S. J. Turco and D. Sacks, *Cell. Microbiol.*, 2010, **12**, 906–918.
58 R. Wilson, M. D. Bates, A. Dostalova, L. Jecna, R. J. Dillon, P. Volf and P. A. Bates, *PLoS Neglected Trop. Dis.*, 2010, **4**, e816.
59 B. J. Walker, R. J. Wheeler, K. Ishimoto and E. A. Gaffney, *J. Theor. Biol.*, 2019, **462**, 311–320.
60 T. D. Serafim, I. V. Coutinho-Abreu, F. Oliveira, C. Meneses, S. Kamhawi and J. G. Valenzuela, *Nat. Microbiol.*, 2018, **3**, 548–555.
61 M. E. Rogers, M. Hajmová, M. B. Joshi, J. Sadlova, D. M. Dwyer, P. Volf and P. A. Bates, *Cell. Microbiol.*, 2008, **10**, 1363–1372.
62 C. Garrett-Jones, *Nature*, 1964, **204**, 1173–1175.
63 V. Seblova, V. Volfova, V. Dvorak, K. Pruzinova, J. Votypka, A. Kassahun, T. Gebre-Michael, A. Hailu, A. Warburg and P. Volf, *PLoS Neglected Trop. Dis.*, 2013, **7**, e2187.
64 M. E. Rogers and P. A. Bates, *PLoS Pathog.*, 2007, **3**, e91.